First-principles study of the electronic structure and magnetism of CaIrO$_3$

Alaska Subedi

Max Planck Institute for Solid State Research, Heisenbergstrasse 1, D-70569 Stuttgart, Germany

I study the electronic structure and magnetism of postperovskite CaIrO$_3$ using first-principles calculations. The density functional calculations within the local density approximation without the combined effect of spin-orbit coupling and on-site Coulomb repulsion show the system to be metallic, which is in disagreement with the recent experimental evidences that show CaIrO$_3$ to be an antiferromagnetic Mott insulator in the $J_{\text{eff}} = 1/2$ state. However, when spin-orbit coupling is taken into account, the Ir t_{2g} bands split into fully filled $J_{\text{eff}} = 3/2$ bands and half-filled $J_{\text{eff}} = 1/2$ bands. I find that spin-orbit coupling along with a modest on-site Coulomb repulsion opens a gap leading to a Mott insulating state. The ordering is antiferromagnetic along the c axis with total moments aligned antiparallel along the c axis and canted along the b axis.

I. INTRODUCTION

Transition-metal oxides (TMOs) in perovskite and related structures exhibit myriad interesting properties. These include unconventional superconductivity in cuprates,[1] colossal magnetoresistance in manganites,[2] and ferroelectricity in Pb(Zr,Ti)O$_3$.[3] In these materials, the transition-metal ion is situated inside an oxygen octahedral cage, which may be arranged in a corner- or edge-shared manner. The interesting properties of TMOs arise because of the competition between the crystal-field splitting (which arises because of covalency between transition metal d and oxygen p states), on-site Coulomb repulsion U, Hund's coupling, spin-orbit (SO) coupling due to orbital degeneracy (leading to unquenched angular moment in the ground state), and different spin-exchange pathways.

In this regard, the discovery of a spin-orbital Mott state in Sr$_2$IrO$_4$ by Kim *et al.*[4,5] is significant because it enables us to study the case where spin-orbit coupling and its interplay with the Coulomb repulsion is an important ingredient in determining the electronic and magnetic properties of the system. Sr$_2$IrO$_4$ exists in a layered perovskite structure. The Ir^{4+} ($5d^5$) ions are situated inside corner-shared O octahedral cages, which are themselves arranged in a square lattice in the ab plane. As there are an odd number of electrons per formula unit, one might expect this material to be a metal in the band picture. However, Sr$_2$IrO$_4$ is experimentally a canted antiferromagnetic insulator.[5] As explained lucidly by Kim *et al.*, a state with an effective total angular momentum $J_{\text{eff}} = 1/2$ that has a complex wave function is realized in Sr$_2$IrO$_4$, which arises due to the combined influence of strong spin-orbit coupling and moderate on-site Coulomb repulsion.[4] A similar conclusion on Sr$_2$IrO$_4$ has been reached through the study of a three-orbital Hubbard model with spin-orbit coupling[6] and combined density functional theory and dynamical mean field theory (LDA+DMFT) calculations,[7] although Arita *et al.* suggest that Sr$_2$IrO$_4$ is a Slater insulator based on their LDA+DMFT study.[8] Interestingly, it was

also found that spin-orbit coupling plays an important role in the electronic properties even for a $4d^5$ system such as Sr$_2$RhO$_4$.[9,10]

It has been suggested that systems in the $J_{\text{eff}} = 1/2$ state, depending on bond geometry, lead to interesting varieties of low-energy Hamiltonians, including the isotropic Heisenberg model and the highly anisotropic quantum compass or Kitaev models relevant for quantum computing.[11] Therefore, it is important to investigate materials that exhibit the $J_{\text{eff}} = 1/2$ state in different structures in order to study the effect of different local environments and spin-exchange pathways. Recently, Ohgushi *et al.* reported resonant x-ray diffraction study of CaIrO$_3$ that indicates this material also exhibits a Mott insulating $J_{\text{eff}} = 1/2$ state.[12] CaIrO$_3$ exists in the postperovskite structure with space group *Cmcm* as shown in Fig. 1. The Ir^{4+} ($5d^5$) ions are situated inside the O octahedra, but these octahedra share an edge along the c axis, unlike the case of Sr$_2$IrO$_4$. Thus, CaIrO$_3$ is another ideal material to investigate the interplay between spin-orbit coupling and on-site Coulomb repulsion that may help in understanding the unique properties that might be exhibited by $J_{\text{eff}} = 1/2$ systems.

Tsuchiya *et al.* have reported first-principles density functional calculations that show this material is a metal within the local density approximation.[13] This is contrary to the experimental evidence that shows this material is a Mott insulator that undergoes an antiferromagnetic transition at $T_{\text{N}} = 115$ K.[14] A recent resonant x-ray diffraction study shows that the ordering is of stripe-type antiferromagnetism along the c axis, with total moments aligning parallel along the a axis and antiparallel along the c axis.[12] The inverse susceptibility $1/\chi$ deviates from the linear behavior at a temperature $\sim$350 K that is considerably higher than T_{N} and a Curie-Weiss fit to χ above 400 K gives a Curie-Weiss temperature of 3900 K.[14] This indicates that the antiferromagnetic correlations arise much before the antiferromagnetic transition, and magnetic ordering is suppressed by low dimensionality or competing ordering interactions. Jang *et al.* have studied the electronic structure of meta-stable perovskite Ca$_{1-x}$Sr$_x$IrO$_3$ ($x = 0, 0.5$,
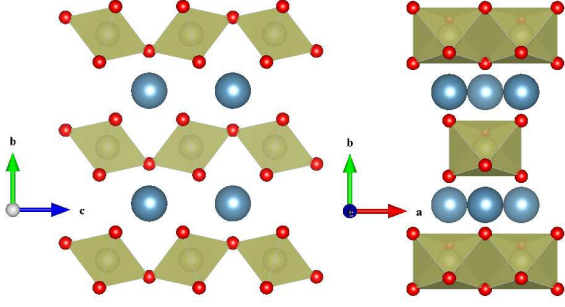
FIG. 1: (Color online) Crystal structure of $CaIrO_3$. The large (cyan) balls are Ca, small (red) balls are O, and the Ir atoms reside inside the (brown) octahedra.
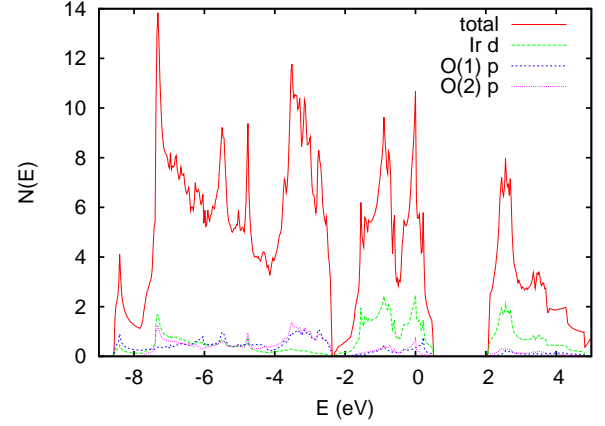

FIG. 2: (Color online) Non-spin-polarized LDA DOS of $CaIrO_3$ (in states/eV). The projections are onto the respective muffin-tin spheres and are only indicative of the contribution to the total DOS. The Fermi energy is at 0 eV.

and 1) thin films using transport measurements, optical spectroscopy, and pseudopotential-based first-principles calculations.[15] They find that perovskite $CaIrO_3$ thin films are semimetallic and near the metal-insulator transition. Their calculations with spin-orbit coupling and on-site Coulomb repulsion U found that the spin-orbit coupling splits the Ir t_{2g} states into $J_{eff} = 3/2$ and $1/2$ states, and $U = 2.0$ eV further splits the $J_{eff} = 1/2$ states, although the valence and conduction bands still touch the Fermi level, resulting in a semimetallic state.

The experimental evidences that have so far been accumulated suggest that calculations that include the effect of spin-orbit coupling and on-site Coulomb repulsion would be helpful in clarifying the electronic and magnetic properties of $CaIrO_3$. In this paper, I report the results of density functional calculations that show $CaIrO_3$ is in a Mott insulating state that is induced by the combined effect of spin-orbit coupling and on-site Coulomb repulsion. This state arises out of spin-orbit split Ir t_{2g} bands that get separated into lower lying fully filled and higher lying half-filled bands that have effective total angular momenta $J_{eff} = 3/2$ and $1/2$, respectively, in the strong spin-orbit coupling limit. The half-filled $J_{eff} = 1/2$ bands are narrow, so even a modest on-site Coulomb repulsion induces a Mott insulating state that is topologically different from the metallic state given by the local density approximation, without taking into account the spin-orbit coupling and on-site Coulomb repulsion. This is a Mott insulating state in the sense that a single-particle theory such as the density functional theory implemented using Kohn-Sham formalism cannot explain the insulating state, and an explicit treatment of on-site Coulomb repulsion is needed. The Mott insulating state thus obtained is antiferromagnetically ordered along the c axis with total moments aligned antiparallel along the c axis and canted along the b axis.

II. APPROACH

The purpose of this paper is to elucidate the role of spin-orbit coupling and on-site Coulomb repulsion on the electronic and magnetic properties of $CaIrO_3$ using density functional calculations. The calculations were performed within the local density approximation (LDA) using the general full-potential linearized augmented plane-wave method as implemented in the ELK software package.[16] Muffin-tin radii of 2.2, 2.0, and 1.6 a.u. for Ca, Ir, and O, respectively, were used. A $8 \times 8 \times 8$ k-point grid was used to perform the Brillouin zone integration, and the convergence of moments was checked on a $10 \times 10 \times 10$ grid. The effect of spin-orbit coupling was treated using a second-variational scheme, and the fully localized limit[17] is used to take into account the double counting in LDA+U calculations. A value for the on-site Coulomb repulsion $U = 2.75$ eV (which gives a band gap close to the experimental value) was used unless otherwise mentioned.

I used the experimental lattice parameters $a = 3.145$ Å, $b = 9.855$ Å, and $c = 7.293$ Å,[18] but relaxed the atomic positions. The calculated atomic positions Ca (0, 0.2498, 0.25), Ir (0, 0, 0), O(1) (0.5, 0.4253, 0.25), and O(2) (0.5, 0.1230, 0.0485) agree well with the experimental values Ca (0, 0.2498, 0.25), Ir (0, 0, 0), O(1) (0.5, 0.4331, 0.25), and O(2) (0.5, 0.1296, 0.0553). The results presented in this paper are for the relaxed atomic positions, but I also performed calculations with experimental atomic positions and came to the same physical conclusions. There are two formula units per primitive unit cell in the $Cmcm$ structure. The Ir^{4+} ions make a two-dimensional rectangular lattice in the ac plane (not shown) and the Ir-O layer is separated by a layer of Ca atoms along the b axis. For the relaxed atomic positions, the O octahedra are tilted by an angle of $22°$. The O octahedra are slightly compressed along the corner-shared O direction (from left to right in the left figure of Fig. 1) with a bond-length ratio of 0.97. The Ir-O distances along the corner-shared c axis and edge-shared a axis are 1.97 and 2.02 Å, respectively.

III. RESULTS

Let us first consider the non-spin-polarized (NSP) LDA calculations. Even though they are inadequate to describe the ground-state properties, these calculations give a decent description of the band structure of $CaIrO_3$ that provide a playground for the interplay between SO coupling and U. The electron density of states (DOS) and band structure for this case are shown in Figs. 2 and 3(a), respectively. Most of the bands along the b direction (Γ-Y) have low dispersion, which suggests that the physics related to two dimensionality might be relevant in this system. There are 24 bands between -9.0 and 1.0 eV. The 18 bands between -9.0 and -2.3 eV (not shown) have a dominant O p character and thus derive from the p orbitals of the six O atoms in the unit cell. These bands also show Ir d character, which implies significant covalency between the O p and Ir d states as the unoccupied Ir d states above Fermi level also contain some admixture of O p states. There is a very small gap of ~ 0.05 eV at -2.36 eV, beyond which lie six bands with a dominant Ir d character. These are the Ir t_{2g} states that are formally antibonding, and these bands correspondingly show some O p contribution. A gap of ~ 1.5 eV separates these t_{2g} states from a group of four bands that have a mostly Ir d character, which are the Ir e_g states. The Ir e_g also have some O p character due to Ir d–O p covalency. The Ir $5d$ states are quite delocalized and the edge-sharing compressed IrO_6 octahedra are rotated by $22°$, and this leads to some hybridization the between Ir t_{2g} and e_g levels. The Ca and Ir s states are high above the Fermi level, and within an ionic limit the electronic structure is consistent with the ionic states Ir^{4+} and O^{2-}, although there is significant deviation from this because of Ir d–O p hybridization. The two Ir^{4+} ions nominally have five electrons each in their d orbitals. As a result, the six Ir t_{2g} bands are not fully filled, and the system is a metal within LDA with a t_{2g} hole on each Ir^{4+} ion.

The metallic state obtained within LDA due to incomplete filling of Ir t_{2g} states is contrary to the experimental evidence that indicates $CaIrO_3$ is a Mott insulator. This suggests that spin-orbit coupling and/or on-site Coulomb repulsion play crucial roles in the electronic and magnetic properties of $CaIrO_3$. Let us now consider the effect of SO coupling and U on the electronic structure of $CaIrO_3$. The NSP LDA, LDA+U, LDA+SO, and LDA+SO+U (with $U = 2.75$ eV) Ir t_{2g} bands are shown in Fig. 3. Let us first note that a value for U of 2.75 eV without the spin-orbit coupling has very little effect on the band structure (I did the calculation with U up to 5 eV without getting an insulating state). This is not surprising as the Ir t_{2g} manifold is spread over a bandwidth of ~ 2.8 eV, and it would require a substantially larger U to open up a gap. However, turning on spin-orbit coupling makes a significant difference in the electronic structure. The system is non-magnetic, so the bands are spin degenerate as they are not exchange split. However, the spin-oribt coupling splits the manifold of six spin-degenerate
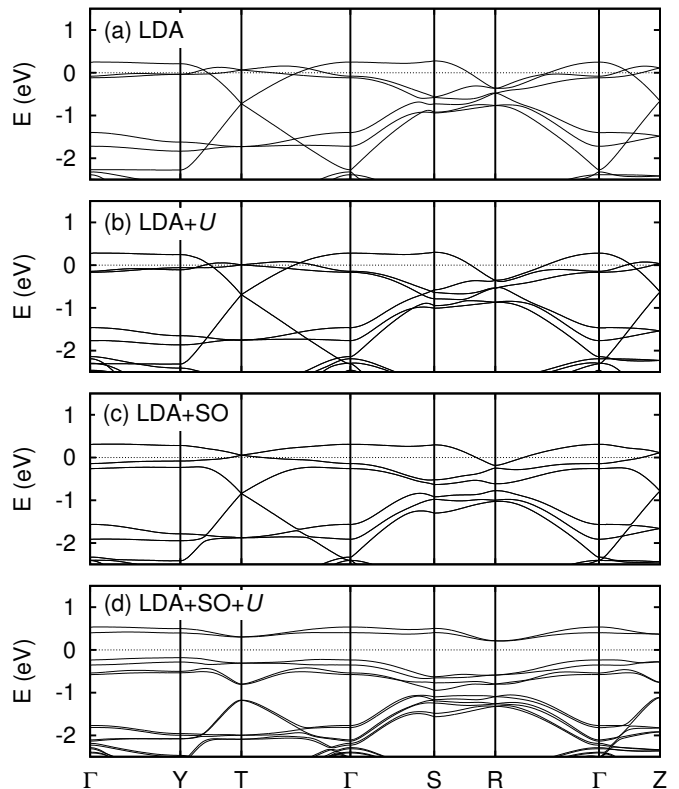

FIG. 3: NSP LDA, LDA+U, LDA+SO and LDA+SO+U band structures, respectively from top to bottom, of $CaIrO_3$. The band structures are plotted along the path Γ (0,0,0) $\rightarrow$ Y $(0,\frac{1}{2},0)$ $\rightarrow$ T $(0, \frac{1}{2}, \frac{1}{2})$ $\rightarrow$ Γ (0,0,0) $\rightarrow$ S $(\frac{1}{4}, \frac{1}{4}, 0)$ $\rightarrow$ R $(\frac{1}{4}, \frac{1}{4}, \frac{1}{2})$ $\rightarrow$ Γ (0,0,0) $\rightarrow$ Z $(0,0,\frac{1}{2})$. Here, $U = 2.75$ eV is used. The bands are exchange split only for the case of LDA+SO+U.

Ir t_{2g} bands into a lower-lying group of four and a higher-lying group of two spin-degenerate bands. In the limit of strong spin-orbit coupling, the lower and higher sets of bands within the t_{2g} manifold would correspond to effective total angular momenta J_{eff} of 3/2 and 1/2, respectively. This is similar to the case of Sr_2IrO_4 where the spin-orbit coupling splits the Ir t_{2g} bands into a lower lying quartet of $J_{eff} = 3/2$ and a higher lying doublet of $J_{eff} = 1/2$ bands.[4] In the case of $CaIrO_3$, the $J_{eff} = 1/2$ bands are narrow with a width of ~ 1 eV. These are separated from the $J_{eff} = 3/2$ bands by ~ 0.15 eV, although the gap is indirect. The ten Ir d electrons in the unit cell completely fill the $J_{eff} = 3/2$ bands, while the $J_{eff} = 1/2$ bands are only half filled. As a result, the system is still metallic.

Even though on-site Coulomb repulsion U and spin-orbit coupling acting alone do not make the system an insulator, it is likely that their combined effect can induce a Mott insulating state by splitting the narrow $J_{eff} = 1/2$ bands. The LDA+SO+U calculations with $U = 2.75$ eV reveal that this scenario is realized in $CaIrO_3$. As shown in Fig. 3(d), the U in the presence of SO coupling makes only minor modifications to the $J_{eff} = 3/2$ bands. The $J_{eff} = 3/2$ bands get exchange split and a

TABLE I: The $\langle \vec{L} \rangle$ and $\langle \vec{S} \rangle$ expectation values computed over Ir muffin-tin spheres and the band gap E_{gap} (eV) for some values of on-site Coulomb repulsion U (eV) and Hund's coupling J (eV). The moments are in units of Bohr magneton.

Site	$\langle \vec{L} \rangle$	$\langle \vec{S} \rangle$	
Ir(1)	$(0.00, 0.06, -0.28)$	$(0.00, 0.03, -0.19)$	$U = 2.75, \; J = 0.0$
Ir(1$'$)	$(0.00, 0.06, 0.28)$	$(0.00, 0.03, 0.19)$	$E_{\text{gap}} = 0.33$
Ir(1)	$(0.00, 0.06, -0.27)$	$(0.00, 0.03, -0.18)$	$U = 2.75, \; J = 0.3$
Ir(1$'$)	$(0.00, 0.06, 0.27)$	$(0.00, 0.03, 0.18)$	$E_{\text{gap}} = 0.30$
Ir(1)	$(0.00, 0.04, -0.18)$	$(0.00, 0.02, -0.13)$	$U = 2, \; J = 0.0$
Ir(1$'$)	$(0.00, 0.04, 0.18)$	$(0.00, 0.02, 0.13)$	$E_{\text{gap}} = 0.03$

degeneracy at the point T $(0, 0.5, 0.5)$ is lifted, but otherwise the bandwidth and topology of the bands do not change substantially. However, the half-filled $J_{\text{eff}} = 1/2$ bands, in addition to being exchange split by $\sim$0.1 eV, are split into the upper (UHB) and lower (LHB) Hubbard bands, yielding a Mott insulating state. The fully occupied $J_{\text{eff}} = 1/2$ LHB has a small bandwidth of $\sim$0.5 eV and is separated from the unoccupied UHB by a gap of $\sim$0.33 eV for $U = 2.75$ eV (the gap is $\sim$0.03 eV for $U = 2$ eV). This agrees well with a band gap of 0.34 eV obtained experimentally.[14,19] I also performed calculations with $U = 1.0, 1.5, 2.0,$ and 2.5 eV. The system is metallic within LDA+SO+U for U up to 1.5 eV, but it becomes an insulator by $U = 2.0$ eV. To see the effect of the Hund coupling J, I did LDA+SO+U calculations with $U = 2.75$ eV and $J = 0.1, 0.2,$ and 0.3 eV. I find that these values of Hund coupling J do not change the qualitative picture—the Ir t_{2g} levels are still split into $J_{\text{eff}} = 3/2$ and $1/2$ bands and the $J_{\text{eff}} = 1/2$ bands are further split into fully occupied LHB and unoccupied UHB. The inclusion of Hund coupling mainly reduces the band gap (for $J = 0.3$ eV, the band gap is 0.30 eV) and the magnetic moment.

The LDA+SO+U calculations give an antiferromagnetic ground state for CaIrO$_3$ along the c axis with total moments aligning antiparallel along the c axis. The orbital and spin moments are parallel to each other along the c axis and ferromagnetically canted along the b axis. The angular and spin expectation values computed over the two Ir muffin-tin spheres Ir(1) (0.0, 0.0, 0.0) and Ir(1$'$) (0.0, 0.0, 0.5) for different U and J values are given in Table I. For $U = 2.75$ eV, the total moment is 0.67 μ_B/Ir with an orbital moment of 0.29 μ_B and a spin moment of 0.38 μ_B $(= 2|\langle \vec{S} \rangle|)$. The canting angle is 10°, approximately half the octahedral tilting angle of 22° and twice the value of 4° reported in Ref. 12. The calculated values differ considerably from what is expected for the ideal $J_{\text{eff}} = 1/2$ state. In the ionic limit, one expects an orbital moment of 0.67 μ_B and a spin moment of 0.33 μ_B for a $J_{\text{eff}} = 1/2$ state.[4] In contrast, I obtain an orbital moment that is lower than the spin moment. The reason for this deviation from the $J_{\text{eff}} = 1/2$ may be the compression and tilting of the IrO$_6$ octahedra, in addition to the co-valency between Ir d and O p states. The compression of the IrO$_6$ octahedra will quench the orbital moment as the degeneracy between t_{2g} states are lifted. Also, the tilting of the IrO$_6$ octahedra causes the e_g bands to get mixed with the t_{2g} states. These two effects should reduce the orbital moment but might enhance the spin contribution. It is interesting to note that Sr$_2$IrO$_4$ also has distortion of the IrO$_6$ octahedra with a bond-length ratio of 1.04 and a tilting angle of 11°,[20] and it has a calculated orbital moment of 0.26 μ_B and spin moment of 0.10 μ_B.[4] As the tilting angle in CaIrO$_3$ is twice that of Sr$_2$IrO$_4$, it might be reasonable to expect that CaIrO$_3$ deviates further from the ideal $J_{\text{eff}} = 1/2$ state due to the mixing of the e_g states.

IV. CONCLUSIONS

In summary, the electronic structure and magnetic properties of CaIrO$_3$ has been studied using first-principles calculations. The system is metallic within the LDA because the Ir t_{2g} states are incompletely filled. Modest values of on-site Coulomb repulsion alone have very little effect on the LDA electronic structure as the Ir t_{2g} states have a broad bandwidth. The introduction of spin-orbit coupling splits the Ir t_{2g} states into fully filled $J_{\text{eff}} = 3/2$ bands and half-filled $J_{\text{eff}} = 1/2$ bands. The half-filled bands have a small bandwidth of $\sim$1.0 eV, which is split into fully filled lower and unfilled upper Hubbard bands by a modest value of on-site Coulomb repulsion. This topologically non-trivial modification of the LDA electronic structure due to the combined effects of spin-orbit coupling and on-site Coulomb repulsion results in a Mott insulating state that is antiferromagnetically ordered along c axis with total moments aligning antiparallel along the c axis and canted along the b axis. For $U = 2.75$ eV, the total magnetic moment is 0.67 μ_B with an orbital contribution of 0.28 μ_B and a spin contribution of 0.38 μ_B. These values differ from what is expected for the ideal $J_{\text{eff}} = 1/2$ state, and this deviation might be explained by the mixing of $J_{\text{eff}} = 1/2$ bands with Ir e_g bands due to the tilting of IrO$_6$ octahedra. There has been great interest in finding different materials with unique magnetic properties. The results presented here give strong support to the claim made by Ohgushi *et al.* in Ref. 12 that CaIrO$_3$ has a unique spin-orbit integrated magnetic ground state.

V. ACKNOWLEDGEMENTS

[1] J. G. Bednorz and K. A. Muller, Z. Phys. B **64**, 189 (1986).

[2] R. von Helmolt, J. Wecker, B. Holzapfel, L. Schultz, and K. Samwer, Phys. Rev. Lett. **71**, 2331 (1993).

[3] B. Jaffe, W. J. Cook, and J. Jaffe, *Piezoelectric Ceramics* (Academic, London, 1971).

[4] B. J. Kim, H. Jin, S. J. Moon, J.-Y. Kim, B.-G. Park, C. S. Leem, J. Yu, T. W. Noh, C. Kim, S.-J. Oh, J.-H. Park, V. Durairaj, G. Cao, and E. Rotenberg, Phys. Rev. Lett **101**, 076402 (2008).

[5] B. J. Kim, H. Ohsumi, T. Komesu, S. Sakai, T. Morita, and H. Takagi, Science **323**, 1329 (2009).

[6] H. Watanabe, T. Shirakawa, S. Yunoki, Phys. Rev. Lett. **105**, 216410 (2010).

[7] C. Martins, M. Aichhorn, L. Vaugier, and S. Biermann, Phys. Rev. Lett. **107**, 266404 (2011).

[8] R. Arita, J. Kuneš, A. V. Kozhevnikov, A. G. Eguiluz, and M. Imada, arXiv:1107.0835.

[9] M. W. Haverkort, I. S. Elfimov, L. H. Tjeng, G. A. Sawatzky, and A. Damascelli, Phys. Rev. Lett. **101**, 026406 (2008).

[10] G.-Q. Liu, V. N. Antonov, O. Jepsen, and O. K. Andersen, Phys. Rev. Lett. **101**, 026408 (2008).

[11] G. Jackeli and G. Khaliullin, Phys. Rev. Lett. **102**, 017205 (2009).

[12] K. Ohgushi, J.-I. Yamaura, H. Ohsumi, K. Sugimoto, S. Takeshita, A. Tokuda, H. Takagi, M. Takata, and T.-H. Arima, arXiv:1108.4523.

[13] T. Tsuchiya and J. Tsuchiya, Phys. Rev. B **76**, 144119 (2007).

[14] K. Ohgushi, H. Gotou, T. Yagi, Y. Kiuchi, F. Sakai, and Y. Ueda, Phys. Rev. B **74**, 241104(R) (2006).

[15] S. Y. Jang, H. Kim, S. J. Moon, W. S. Choi, B. C. Jeon, J. Yu, and T. W. Noh, J. Phys.: Condens. Matter **22**, 485602 (2010).

[16] http://elk.sourceforge.net

[17] V. I. Anisimov, I. V. Solovyev, M. A. Korotin, M. T. Czyżyk, and G. A. Sawatzky, Phys. Rev. B **48**, 16929 (1993).

[18] R. von Fritz and B. Dietrich, Z. Anorg. Allg. Chem. **336**, 17 (1965).

[19] In Ref. 14, the resistivity versus temperature curve is fit to the formula $\rho(T) = A \exp(\Delta/T)$ and a value of $\Delta = 0.17$ eV is obtained. The band gap should be twice the value of Δ, i.e. 0.34 eV.

[20] M. K. Crawford, M. A. Subramanian, R. L. Harlow, J. A. Fernandez-Baca, Z. R. Wang, and D. C. Johnston, Phys. Rev. B **49**, 9198 (1994).